Author Manuscript

Author Manuscript

Author Manuscript

Author Manuscript

HHS Public Access

Author manuscript

*J Proteome Res*. Author manuscript; available in PMC 2019 June 13.

Published in final edited form as:

*J Proteome Res*. 2018 September 07; 17(9): 3268–3280. doi:10.1021/acs.jproteome.8b00379.

# Ron Receptor Signaling Ameliorates Hepatic Fibrosis in a Diet-Induced Nonalcoholic Steatohepatitis Mouse Model

**Joselyn Allen**, **Jingtao Zhang**, **Michael D. Quickel**, **Mary Kennett**, **Andrew D. Patterson**[*], and **Pamela A. Hankey-Giblin**[*]

Department of Veterinary and Biomedical Sciences, The Pennsylvania State University, University Park, Pennsylvania United States

## Abstract

Liver fibrosis is commonly observed in the terminal stages of nonalcoholic steatohepatitis (NASH) and with no specific and effective antifibrotic therapies available, this disease is a major global health burden. The MSP/Ron receptor axis has been shown to have anti-inflammatory properties in a number of mouse models, due at least in part, to its ability to limit pro-inflammatory responses in tissue-resident macrophages and hepatocytes. In this study, we established the role of the Ron receptor in steatohepatitis-induced hepatic fibrosis using Ron ligand domain knockout mice on an apolipoprotein E knockout background (DKO). After 18 weeks of high-fat high-cholesterol feeding, loss of Ron activation resulted in exacerbated NASH-associated steatosis which is precedent to hepatocellular injury, inflammation and fibrosis. $^{1}$H nuclear magnetic resonance (NMR)-based metabolomics identified significant changes in serum metabolites that can modulate the intrahepatic lipid pool in hepatic steatosis. Serum from DKO mice had higher concentrations of lipids, VLDL/LDL and pyruvate, whereas glycine levels were reduced. Parallel to the aggravated steatohepatitis, increased accumulation of collagen, inflammatory immune cells and collagen producing-myofibroblasts were seen in the livers of DKO mice. Gene expression profiling revealed that DKO mice exhibited elevated expression of genes encoding Ron receptor ligand MSP, collagens, ECM remodeling proteins and pro-fibrogenic cytokines in the liver. Our results demonstrate the protective effects of Ron receptor activation on NASH-induced hepatic fibrosis.

## Graphical Abstract

[*]**Corresponding Authors** (P.A.H.-G.) Tel: 814-863-0128. Fax: 814-863-6140. phc7@psu.edu., (A.D.P.) Tel: 814-867-4565. adp117@psu.edu.

Author Contributions

J.A., A.D.P., P.H.-G. conceived and designed research. J.A. performed experiments. J.Z. performed NMR acquisition and analysis. M.D.Q performed experiments necessary for manuscript revisions. M.K. performed the histopathologic scoring. J.A., A.D.P., P.H.-G. interpreted results of experiments. J.A. drafted manuscript. J.A., A.D.P., and P.H.-G. edited and revised the manuscript. A.D.P. and P.H.-G. approved final version of manuscript.

The authors declare no competing financial interest.

ASSOCIATED CONTENT

Supporting Information

The Supporting Information is available free of charge on the ACS Publications website at DOI: 10.1021/acs.jproteo-me.8b00379. Detailed methods of the $^{1}$H NMR Spectroscopy acquisition and analysis. Table S-1. $^{1}$NMR signal assignments of serum metabolites (PDF)

Author Manuscript Author Manuscript Author Manuscript Author Manuscript

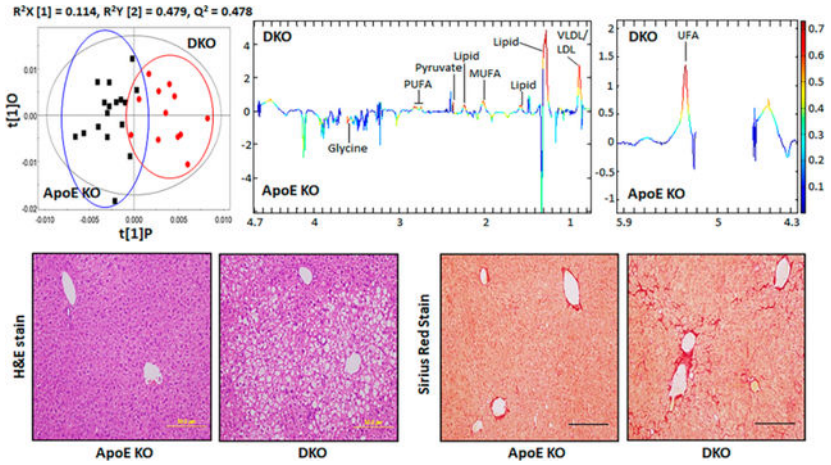


**Keywords**

ron receptor; MSP; liver fibrosis; NASH; metabolomics

## INTRODUCTION

In the United States the prevalence of nonalcoholic fatty liver disease (NAFLD) is estimated at 25%. The steady rise in cases is assumed to parallel the obesity epidemic.[1,2] Further aggravation of fatty liver disease by additional intrinsic insults such as inflammation and oxidative stress promote high-risk nonalcoholic steatohepatitis (NASH) which can progress to hepatic fibrosis and eventually cirrhosis.[1,3] In the U.S, NASH affects 25% of patients with NAFLD (5–6% of U.S. adults) and within that NASH population 25% (1–2% of US adults) experience more advanced stages which trigger irreversible liver injury, scarring and failure.[4] Liver fibrosis marks the detrimental turning point of sustained liver injury in NASH, an irreversible consequence of overly active wound healing in response to acute and chronic liver damage. The poor prognosis of advanced steatohepatitis has resulted in its emergence as a major cause of liver disease morbidity and mortality worldwide.[5–9] Because of the high risks associated with NASH, including the development of fibrosis, current research efforts are directed toward understanding the intricate molecular pathways facilitating the onset and progression of the NASH spectrum. Although many strides have been made to better understand the progression of NASH, effective treatments that specifically target NASH and associated hepatic fibrosis are not yet available. In this study, we explored the effects of a potential therapeutic target for treating steatohepatitis-induced fibrosis.

Recepteur d'Origine Nantais (RON) is a receptor tyrosine kinase (RTK) belonging to the MET proto-oncogene family. The ligand for RON is macrophage stimulating protein (MSP), also known as hepatocyte growth factor-like protein (HGFL). We have shown previously that the activation of RON by MSP promotes anti-inflammatory responses in tissue-resident macrophages and other groups have shown similar effects in hepatocytes.[10–16] When activated by MSP, the biological function of Ron is primarily mediated by a two-tyrosine docking site, which recruits the adaptor, growth factor receptor-bound protein 2 (Grb2). Recruitment of the large scaffolding protein, Grb2-associated binding protein 1 (Gab1), is

Author Manuscript Author Manuscript Author Manuscript Author Manuscript

mediated by Grb2 and a unique Met binding domain (MBD) which promotes the interaction of Gab1 with Met and Ron.[11,17–19] Gab1 has been shown to have antifibrotic function in a carbon tetrachloride ($CCL_4$)-induced liver fibrosis mouse model through its anti-inflammatory and reparative properties.[20] Other studies have demonstrated that the upstream Met receptor also mitigates hepatic fibrogenesis in methionine-choline deficient diet (MCD)- and $CCL_4$-induced mouse models.[21,22] Collectively, these findings gave us the incentive to investigate the effects of Ron on hepatic fibrosis. In previous studies, we have shown that Ron receptor signaling suppresses steatosis, hepatocellular injury and inflammation in a diet-induced model of NASH.[14] However, the potential effects of Ron on hepatic fibrosis was unexplored.

In this study, we report the effects of Ron on liver fibrosis using a steatohepatitis mouse model subjected to high caloric feeding. Following administration of a high-fat high-cholesterol diet, our mice rapidly developed advanced steatohepatitis with pathology characteristics which mimics those found in humans with advanced NASH including steatosis, infiltrated inflammatory immune cells, hepatocellular damage and fibrosis. Our results show that mice with a targeted deletion of the Ron ligand binding domain were more prone to the development of fibrosis. The pro-fibrotic effects of Ron deficiency were mediated by metabolic abnormalities, increased infiltration of immune cells, enhanced hepatic stellate cell activation, as well as upregulated expression of extracellular remodeling proteins and inflammatory cytokines/chemokines. This study supports a critical role of Ron in mitigating hepatic fibrosis in the context of NASH.

## MATERIALS AND METHODS

### Chemical Reagents and Antibodies

$D_2O$ was purchased from Cambridge Isotope Laboratories Inc. (Miami, FL). Antirat F4/80 antibody was obtained from AbD Serotech (Raleigh, NC). Antirabbit aSMA antibody was obtained from Abcam (Cambridge, MA). Secondary antibodies goat antirat IgG, goat antirabbit IgG and tertiary antibody antigoat streptavidin horseradish peroxidase (HRP) were purchased from Vector Laboratories (Burlingame, CA)

### Animal Model and Diet

Male mice, six-week-old of age that are deficient for apolipoprotein E (ApoE KO) were housed in temperature-controlled room at 22 °C and 60% relative humidity with 12 h light/dark cycle throughout the experiment. Mice with a targeted deletion of the ligand binding domain of Ron (Ron KO) were crossed with ApoE KO mice to generate Ron receptor Apolipoprotein E double knockout mice (DKO). Male ApoE KO and DKO mice on a C57BL/6 background were housed 2–3 mice per cage and fed a high-fat high-cholesterol diet (HFHCD) [60% fat and 1.25% cholesterol] for 18 weeks. The cholesterol enriched high-fat diet was purchased from Bioserv (F6334; Flemington, NJ). Concluding the 18-week diet regimen, mice were euthanized by $CO_2$ asphyxiation. All experimental protocols used in this study were approved by the Pennsylvania State University Institutional Animal Care and Use Committee.

Author Manuscript Author Manuscript Author Manuscript Author Manuscript

### Histopathological Examination

Livers were rapidly excised, weighed, and aliquots were stored accordingly. Livers were snap-frozen in liquid nitrogen and stored at −80 °C for quantitative real-time PCR (qRT-PCR). Additional liver tissues were fixed in 10% formalin for hematoxylin-eosin (H&E) staining or immunohistochemistry. H&E staining was performed on fixed paraffin embedded livers by Histoserv, Inc. (Germantown, MD). Paraffin blocks were prepared as 5 μm cross sections for H&E staining and Sirius red staining. Images of stained liver sections were captured at 20× magnification on bright-field microscope (Olympus BX51) for analysis. Representative images were captured at 10× magnification. Grading of steatohepatitis and hepatic fibrosis was performed blindly by a board-certified laboratory animal veterinarian with training in pathology. The degree of steatohepatitis was evaluated using the following scoring system (0 = no lesions; 1 = few or scattered lesions affecting <10% of the tissue; 2 = mild lesions affecting 10–20% of the tissue, 3 = moderate lesions affecting 20–30% of the tissue; 4 = severe lesions affecting >30% of the tissue). Histological grading of liver fibrosis was performed using the following system (1 = normal to minimal fibrosis, with lesions primarily around portal triads and central veins; 2 = mild fibrosis; lesions primarily surrounding portal triads and central veins with occasional focal areas of fibrosis in parenchyma; 3 = moderate fibrosis, lesions abundantly surrounding portal triads, centrals veins, and in parenchyma).

### Biochemical Tests

Blood was obtained through exsanguination of the heart and collected in serum separator tubes. The clot was removed by centrifugation at 14 000g for 10 min. Serum was stored in −80 °C until further use. 50–100 μL of blood serum was used to detect the concentration of alanine aminotransferase (ALT), aspartate aminotransferase (AST), total bilirubin (TBIL), albumin (ALB), alkaline phosphatase (ALP), globulin (GLOB) and total protein (TP) using the IDEXX VetTest Chemistry Analyzer coupled with the IDEXX VetLab Station Laboratory Information Management System available at the Pennsylvania State University Central Biological Laboratories.

### $^{1}$H Nuclear Magnetic Resonance (NMR)

To prepare serum samples for $^{1}$H NMR analysis, 200 μL of serum and 400 uL of saline solution containing 50% $D_20$ were mixed. Samples were then briefly vortexed and centrifuged at 11 180g for 10 min at 4 °C and 550 μL of the supernatant was transferred to 5 mm NMR tubes. $^{1}$H NMR spectra of serum was acquired as previously described.[23,24] Spectral data processing and multivariate analysis was performed as previously described.[23,24]

### Immunohistochemical Examination

Standard immunohistochemical (IHC) staining of 5 μm cross-sectioned liver tissue was performed by Histosev Inc. (Germantown, MD). Kupffer cells were detected using a primary antirat F4/80 antibody (1:50). To visualize hepatic stellate cell (HSC) activation, a primary antirabbit aSMA antibody was used (1:100). Primary antibody stained sections were

Author Manuscript Author Manuscript Author Manuscript Author Manuscript

incubated with the secondary antibody goat antirat IgG or goat antirabbit IgG at a 1:5000 dilution followed by an antigoat streptavidin HRP conjugated antibody.

### Quantitative RT-PCR Analysis

Whole liver samples were pulverized using a tissue homogenizer in RiboZol RNA Extraction Reagent (Ameresco; Solon, OH) as instructed by the manufacturer. RNA concentration was quantified using a Nanodrop spectrometer at an absorbance of A260. Using 2 $\mu$g of RNA, cDNA was synthesized using the High Capacity Reverse Transcription Kit (Applied Biosystems; Foster City, CA). The cDNA was assessed for gene expression using FAM-labeled Taqman probes (Applied Biosystems; Foster City, CA). Real time PCR was performed on the 7900HT Fast Real-Time PCR System (Applied Biosystems Foster City, CA). Threshold cycle values were normalized to the housekeeping gene *Gapdh.*

### Statistical Analyses

Values are represented as mean ± SEM. Statistical significance was determined using the two-tailed Student's *t* test at a threshold of 0.05, unless stated otherwise. Significant differences are represented as the following, $*p < 0.05$, $**p < 0.01$, $***p < 0.001$, $****p < 0.0001$. All analyses were performed using GraphPad Prism 7.0 (San Diego CA).

## RESULTS

### Ron Receptor Deficiency Accelerates Diet-Induced Liver Steatosis

To evaluate the effects of the Ron receptor on steatosis associated with nonalcoholic steatohepatitis, C57BL/6 male double knockout (DKO) mice generated by breeding apolipoprotein E deficient (ApoE KO) mice with mice lacking the ligand binding domain of the Ron receptor (Ron KO) were used in this study (Figure 1A). DKO animals and ApoE KO control mice were maintained on a high-fat high-cholesterol diet (HFHCD) for 18 weeks (Figure 1A). Ron receptor deficiency resulted in increased incidence of severe steatosis in DKO mice (Figure 1C, E, and F) with no differences in body weights (Figure 1B), liver weights and liver to body weight ratios (Figure D) between ApoE KO and DKO mice at 18 weeks following HFHCD feeding. Evaluation of H&E stained liver cross sections showed a higher total pathology score which included histological grading of hepatocellular vacuolation, lipidosis, inflammation and hepatocyte karyomegaly (Figure 1F). The gross assessment of nonalcoholic steatohepatitis showed that livers from DKO mice frequently exhibited moderately afflicted tissue (Score 3, 20–30%) when compared to ApoE KO control mice, whereas control mice more frequently demonstrated less severe or fewer affected tissue area (Score 1, <10%) (Figure 1F). Histological analysis demonstrated that DKO livers exhibited increased prevalence of lipidosis with both macro- and micro-vesicular steatosis present, which extensively accumulated in the hepatic parenchyma (Figure 1E and F). Livers from DKO mice also showed a higher frequency of hepatocytes enlarged by large fat globules that displaced their nuclei. In DKO mice, this pathology affected the liver tissue more extensively as shown by higher histological scores (3, 20–30%; 4, >30%), whereas livers from ApoE KO mice tended to show minimal (Score 1, <10%) to no affliction (Figure 1F). Glycogen vacuolation of nuclei, another common characteristic of NASH, was also more frequently observed in DKO livers and more commonly affected larger areas of the

Author Manuscript Author Manuscript Author Manuscript Author Manuscript

tissue (Score 3, 10–30%; 4, >30%) (Figure 1F). Livers from DKO mice also exhibited increased incidences of karyomegalic (with enlarged nuclei) hepatocytes often associated with hepatocellular degeneration (Figure 1F). In support of the exacerbated NASH pathology observed in DKO animals, serological markers of liver damage alanine aminotransferase (ALT) and aspartate aminotransferase (AST) were significantly increased (Figure 1G). Other biochemical markers for liver disease including total bilirubin (TBil), albumin (ALB) globulin (Glob) and total protein (TP) were also higher in DKO animals when compared to ApoE KO mice (Figure 1G).

## Ron Deficiency Alters Serum Metabolic Parameters

$^1$H Nuclear magnetic resonance (NMR) was used to assess the metabolic profile of blood sera from ApoE KO and DKO mice (Figure 2). The OPLS-DA score plot ($R^2X = 0.114$, $R^2Y = 0.479$, $Q^2 = 0.478$) showed that sera from ApoE KO and DKO mice clearly clustered into two groups (Figure 2A). In this study, the OPLS-DA model was validated by a permutation test with 7 permutations (Figure 2B). Analysis of the OPLS coefficient and statistical analysis showed that 8 metabolites responsible for the differentiation crossed the level statistical significance at P value <0.05 (Figure 2C,D, and Supporting Information (SI) Table S1). According to the correlation coefficient loading plot, loss of Ron activation in DKO mice resulted in the relative contents of circulating lipids, pyruvate and very-low density lipoprotein (VLDL)/low density lipoprotein (LDL) to be significantly higher than that in ApoE KO sera (Figure 2C,D, and SI Table S1). Alternatively, the relative content of glycine was decreased in DKO sera (Figure 2C,D, and SI Table S1). The augmented serum levels of lipids in DKO animals may in part contribute to the increased intrahepatic lipid accumulation observed in these animals. (Figure 2C,D, and Table S1)

## Ron Receptor Deficiency Accelerates Hepatic Fibrosis in a Diet-Induced NASH Model

Advanced steatohepatitis is a major cause of liver fibrosis, therefore we investigated whether loss of Ron receptor signaling affected fibrosis development and progression in this model. To evaluate the severity of fibrosis in livers from diet-fed animals, the localization and distribution of Sirius red-stained collagen fibers were evaluated. Blinded histochemical grading of Sirius red-stained liver sections revealed that HFHCD-fed DKO animals exhibited more severe fibrotic lesions when compared with livers from ApoE KO animals (Figure 3A and B). DKO livers frequently exhibited mild (Score 2, 41.7%) or moderate fibrosis (Score 3, 58.3%) with fibrotic lesions accumulating around portal triads and veins and in the parenchyma (Figure 3A and B). Alternatively, HFHCD-fed ApoE KO mice more frequently showed minimal to no fibrosis (Score 1, 38.5%) or mild fibrosis (Score 2, 53.8%) and were less likely to exhibit moderate fibrosis (Score 3, 7.7%) (A and B). Quantification of collagen accumulation demonstrated that DKO livers exhibited a strong increase in Sirius red positive areas, when compared to livers from ApoE KO control mice (Figure 3A and C). To assess the transcriptional profile of fibrogenesis in these animals, we analyzed the expression of tissue remodeling genes in livers derived from HFHCD-fed mice, including type I collagen *(Col1a1, Col1a2)*, type 3 collagen *(Col3a1)*, type 4 collagen *(Col4a1)*, matrix metalloproteinase —2 *(Mmp2)*, matrix metalloproteinase-9 *(Mmp-9)*, tissue inhibitor of metalloproteinase-1 *(Timp-1)*, and inhibitor of metalloproteinase —2 *(Timp-2).* Livers from DKO mice exhibited a significant increase in the expression levels of *Col1a1, Col1a2,*

Author Manuscript Author Manuscript Author Manuscript Author Manuscript

*Col1a3*, and *Col4a1*, supporting the histological findings (Figure 3D). Alternatively, we observed downregulated hepatic expression of fibronectin in these mice (Figure 3D). Expression levels of *Mmp-2* and *Timp-1* were drastically elevated in DKO livers, whereas *Mmp-9* was significantly decreased in these animals (Figure 3E).

## Ron Receptor Deficiency Results in Increased Hepatic Expression of MSP, Profibrogenic Genes, And Hepatic Stellate Cell Activation

Liver injury has shown to increase the expression of growth factors, including MSP (or HGFL), to facilitate liver regeneration and regulate inflammation which is essential for the maintenance of important hepatic functions.[25–27] The increased level of this mitogenic growth factor is thought to reflect the degree of liver dysfunction during chronic hepatic injury. In accordance with the literature, the level of expression for MSP mRNA was increased in livers from DKO mice when compared to that of ApoE KO control mice (Figure 4A). Several cytokines are central to the onset and progression of fibrosis, including platelet derived growth factor (PDGF), connective tissue growth factor (CTGF) and transforming growth factor $\beta$ (TGF$\beta$). The expression of genes encoding the cytokines TGF$\beta$ and PDGFs ($\alpha$ and $\beta$), which are potent activators and mitogens of HSCs, was upregulated in livers from DKO mice (Figure 4A). Similarly, *Ctgf* expression which is known to regulate ECM gene expression, as well as HSC migration and proliferation, was also higher in DKO livers (Figure 4A). The PDGF receptors, PDGFR$\alpha$ and PDGFR$\beta$, are primarily expressed by hepatic stellate cells (HSCs) and are often upregulated in liver fibrosis. In DKO livers, the expression of *Pdgfr-*$\beta$, but not *Pdgfr-*$\alpha$, was elevated when compared to control ApoE KO mice (Figure 4A). To determine whether HSC activation was increased in DKO livers, immunohistochemistry was performed on liver sections to detect $\alpha$SMA, a key marker for HSC activation. Quantification of $\alpha$SMA in immunostained liver sections revealed that DKO animals exhibited increased accumulation of $\alpha$SMA positive cells (Figure 4B and C). Significantly elevated hepatic mRNA expression of *$\alpha$Sma* in DKO animals further corroborated these findings (Figure 4D). Our results suggest that loss of Ron in a diet-induced NASH model augments pro-fibrogenic transcriptional programs that could positively regulate stellate cell activation, proliferation, and survival.

## DKO Animals Exhibit Increased Immune Cell Recruitment and Inflammation in Fibrotic Livers

Persistent tissue damage, as a result of chronic steatosis, provokes the recruitment of immune cells, facilitates HSC activation, and initiates liver fibrosis. Histological analysis of H&E stained liver sections demonstrated greater numbers of inflammatory foci in the livers of diet-fed DKO animals (Figure 5A and B). On average, 10–20% (Score 2) of the DKO liver was infiltrated by immune cells. Immune cell infiltrates that affected 20–30% (Score 3) of the liver were also frequently observed in DKO animals. Alternatively, ApoE KO animals exhibited minimal to mild infiltration affecting either <10% (Score 1) or 10–20% (Score 2) of the liver (Figure 5B). Previously, we have shown that loss of Ron receptor signaling affects Kupffer cell heterogeneity, however macrophage infiltration was not previously assessed. Following 18 weeks of HFHCD feeding, livers from DKO mice exhibited significantly higher mRNA expression of Kupffer cell/macrophage markers including F4/80, CD68 and CD11c (Figure 5C). Upregulation of *Ly6c* transcript expression, a monocyte

Author Manuscript Author Manuscript Author Manuscript Author Manuscript

marker, was also observed in DKO livers when compared to ApoE KO control animals (Figure 5C). Because macrophages are the primary source of inflammation in steatohepatitis and fibrosis, we analyzed macrophage recruitment in these livers. Toward that end, immunohistochemistry for F4/80 was performed on liver cross sections from these HFHCD-fed animals (Figure 5D). Our analysis concluded that DKO livers harbored elevated intrahepatic accumulation of $F4/80^{+}$ Kupffer cells when compared to control animals (Figure 5E).

A consequence of intrahepatic immune cell recruitment is chronic inflammation which plays a crucial role in triggering pro-fibrogenic events. Significant elevation in the mRNA expression of the pro-inflammatory cytokines *Tnfα* and *Il-12b* was detected in livers from DKO animals when compared to ApoE KO controls, whereas expression of *Inos* remained unchanged (Figure 5F). Interestingly, loss of Ron receptor signaling resulted in a significant downregulation of *Il-1β* expression in DKO livers (Figure 5F). TLR4 mediated inflammation has been acknowledged as a critical factor for both the onset and progression of liver fibrosis. In livers from DKO mice, *Tlr4* expression was significantly upregulated (Figure 5F). The expression of relevant chemokines and their receptors was also measured given the increased recruitment of immune cells (ICs) observed in DKO livers. In agreement with the increased recruitment of ICs, mRNA levels of *Cxcl2/Mip2, Ccl2* and *Ccr2* were drastically upregulated in the livers of HFHCD-fed DKO mice (Figure 5F). We also examined the expression of macrophage-specific anti-inflammatory marker, *Ym-1*, in whole liver extract from HFHCD-fed mice. *Ym-1* gene expression was reduced in DKO livers (Figure 5F). These results highlight the exaggerated levels of inflammation in the liver, a major risk factor for liver fibrosis, when Ron signaling is disrupted.

## DISCUSSION

The onset and pathogenesis of hepatic fibrosis relies on dramatic changes to the extracellular matrix microenvironment through the actions of inflammatory insults elicited during steatohepatitis. Steatohepatitis progresses to fibrosis in response to inflammatory signals released by damaged hepatocytes and recruited immune cells.[3,28] The effects of these pro-fibrogenic insults can be seen as excessive wound healing responses marked by the increased deposition of extracellular matrix components.[3,28–30] Activation of stellate cells by cytokines including PDGF, TGFβ, and CTGF transforms these cells to myofibroblasts that synthesize ECM components such as collagens (Type I, III, IV), fibronectin, and hyaluronic acids.[31–33] In stellate cells, activation upregulates the expression of key fibrogenic target genes encoding cytokines (TGFβ, CTGF, PDGFs), chemokines (CCR2, CCL5, MIP-2), growth factor receptors, cytoskeletal proteins (αSMA), extracellular matrix components and ECM remodeling proteins (MMP-2, MMP-9, TIMP-1).[33,34] These pro-fibrogenic events are highly regulated by the secretion of cytokines such as TNFα, IL-6, CCL2, IL-1, PDGFs, and TGFβ by recruited and tissue-resident macrophages.[3,30,35–40] Altogether, fibrogenesis is driven by the interactions between stellate cells and inflammatory signals which act to launch a cascade of pathophysiological events crucial in establishing and maintaining liver fibrosis.

Author Manuscript Author Manuscript Author Manuscript Author Manuscript

In this study, we provide evidence that deletion of the ligand binding domain of Ron results in enhanced liver fibrosis in a diet-induced steatohepatitis mouse model. Our observations confirm the critical role of Ron receptor signaling in the pathophysiology of NASH-associated hepatic fibrosis. Dietary feeding of ApoE KO rodents induced the development of hepatic fibrosis that mimics the progression of human NASH. The loss of Ron receptor activation resulted in exacerbated pathological characteristics of advanced steatohepatitis. This aggravated phenotype included increased steatosis, immune cell infiltrates, karyomegaly, hepatocellular vacuolation and hepatocyte damage marked by elevated ALT and AST levels. Diet-induced liver disturbances often trigger alterations in glycolysis which can cause a rise in circulating pyruvate.[41] This may explain the elevated pyruvate levels in DKO sera. In DKO sera, our $^{1}$H NMR analysis revealed that glycine levels were lower than that in ApoE KO sera which supports findings from other studies. In multiple studies, it has been shown that NASH patients have reduced levels of glycine in the plasma.[42–45] Moreover, glycine treatment was shown to have ameliorative effects on NASH and hepatic fibrosis in rodent models.[46–48] The nonessential amino acid, glycine, inactivates hepatic macrophages or Kupffer cells by blunting cytokine production and antagonizes apoptosis of sinusoidal endothelial cells in the liver.[49] These events are crucial in the development of NASH and hepatic fibrosis.

A main source of stored intrahepatic fat relies on the uptake of circulating lipids into the liver. Our rodent model demonstrated that loss of Ron activation resulted in increased circulation of lipids, which suggests that the lipid-rich metabolic profile of DKO animals may contribute to the increased accumulation of intrahepatic fat observed in these mice (Figure 6). Lipid uptake into the liver and storage as triglycerides (TG) is associated with enhanced TG mobilization through VLDL secretion by the liver. This may explain the increased circulating levels of VLDL (the major carrier of serum TG) in DKO animals. Of note, the availability of VLDL and LDL play a crucial role in initiating atherosclerotic lesions through the retention of these lipid-rich lipoproteins in the subendothelial space of the arterial wall.[50] Along those lines, in a previous study using this diet-induced rodent model, we demonstrated that the progression of atherosclerosis was accelerated in mice lacking Ron receptor signaling. DKO mice exhibited more extensive atherosclerotic plaques when compared to ApoE KO control animals.[14]

The exacerbated steatohepatitis in DKO mice was paralleled by accelerated hepatic fibrosis. In livers from DKO animals, fibrotic lesions were more frequently developed and deposition of scarred tissue was most abundant surrounding portal triad and central vein and throughout the parenchyma. Immunohisto-chemistry of $\alpha$SMA confirmed that the aggravation of liver fibrosis in DKO animals was due to the enhanced activation of hepatic stellate cells (HSCs). The activation of stellate cells was also implicated by the higher expression of pro-fibrogenic markers including *Pdgf-a, Pdgf-b, Pdgfr-β, Ctgf*, and *Tgfβ* in DKO livers. These growth factors are potent inducers of collagen production, consistent with the increased accumulation of Sirius red-stained collagen and upregulated collagen genes *(Col1a1, Col1a2, Col3a1, Col4a1)* in DKO livers. Alternatively, the expression of the ECM glycoprotein, fibronectin, was significantly decreased. Fibronectin has been shown to reduce the availability of active TGF$\beta$ and thus reduce fibrogenesis by decreasing HSC responsiveness to TGF$\beta$.[51,52] The protective function of fibronectin can thus explain the

Author Manuscript Author Manuscript Author Manuscript Author Manuscript

trend observed in the livers of DKO mice. In fibrogenesis, the replacement of normal ECM with fibrillar, contractile ECM is a key event in the initiation of liver scarring. Dynamic changes in the expression of MMPs and TIMPs in injured livers regulate extracellular matrix remodeling in liver fibrosis.[53–55] In agreement with this, *Mmp-2* and *Timp-1* expression was upregulated in highly remodeled fibrotic DKO livers. Alternatively, *Mmp-9* expression was downregulated in livers from these mice. Active recombinant MMP-9 has been demonstrated to induce apoptosis of stellate cells *in vitro*, and overexpression of *Mmp-9 in vivo* was able to reduce collagen content in the liver.[56–59]

Inflammation is a main executor of fibrogenesis, facilitating the activation, proliferation and survival of hepatic stellate cells. It is regulated by the actions of cytokines that are released by immune cells infiltrating into the injured liver. In the highly fibrotic livers of DKO animals, immune cell infiltrates were increased. In agreement with these findings, higher expression of leukocyte markers *Ly6c, F4/80.* and *CD68* was also observed in DKO livers. The altered expression of the macrophage markers, *F4/80* and *CD68*, suggests that there was increased trafficking of macrophages into the liver. Immunohistochemistry of F4/80 corroborated our gene expression findings, where livers from DKO mice exhibited increased accumulation of F4/80$^+$ Kupffer cells (KCs). The expression of the Ml marker, *CD11c*, was elevated in DKO livers. These results are consistent with our previous observations that Ron alters the balance of macrophage activation in the progression of nonalcoholic hepatosteatosis.[14] Taken together, these results suggest that there is a shift in the polarization of macrophage populations in the absence of Ron activation.

Kupffer cells represent the largest macrophage population among all tissues. [35,60,61] Maintenance of liver function, in part, relies on tightly regulating a balance of macrophage phenotypes. As a result, the dominating phenotype of macrophages plays a major role in dictating the pathogenesis of liver fibrosis. Liver fibrosis pathogenesis depends on a prevailing pro-inflammatory (Ml) macrophage phenotype which facilitates the activation and survival of HSCs by promoting the release of specific growth factors and cytokines. [35–38,62,63] In previous studies, we characterized different KC populations isolated from HFHCD-fed ApoE KO animals. CD11c$^+$ Ml-like KCs exhibited decreased expression of Ron, whereas M2-like KCs lacking CD11c expression exhibited higher expression of Ron.[14] KCs lacking Ron expression exhibited a M1-like phenotype marked by increased INOS expression.[14] Alternatively, KCs expressing Ron exhibited higher expression of the M2 marker, Arginase I.[14] Several studies point to the antifibrotic role of arginase I-expressing macrophages, and depletion of arginase I-expressing macrophages was shown to exacerbate the development of liver fibrosis.[39] Collectively, our findings suggest that Ron receptor expression and signaling corresponds to a reparative (M2) macrophage phenotype which is protective in liver disease. Therefore, Ron receptor signaling may act to curb inflammatory responses, promote the restoration of tissue integrity following liver injury, and thus retards the development of liver fibrosis (Figure 6). Consistent with this notion, we demonstrated that ApoE KO control mice exhibit reduced hepatic expression of pro-inflammatory markers *(Tnfa, Il-12b, Tlr4)* and chemokines *(Cxcr2/Mip-2, Ccl2, Ccr2, Ccl5/Rantes).* Alternatively, ApoE KO mice showed higher expression of macrophage-specific M2 marker, *Ym-1.* These results are in agreement with findings from our previous study.[14] Because Ron was shown to restrain further aggravation of steatohepatitis by limiting steatosis, hepatocellular damage

Author Manuscript Author Manuscript Author Manuscript Author Manuscript

and inflammation,[14] we speculate that the ability of Ron to mitigate these events protects against liver fibrosis.

Receptor tyrosine kinases have long been implicated in antifibrotic events; however, the effects of Ron activation on hepatic fibrosis in a diet-induced model were not previously investigated. The Gab1 adaptor protein, involved in signaling downstream of the Met and Ron receptors, has been shown to regulate pro-fibrotic chemokine CCL5 synthesis in hepatocytes.[20] Loss of hepatocyte-specific Gab 1 resulted in increased CCL5 synthesis, increased macrophage infiltration and accelerated liver fibrosis.[20] Met was also shown to protect against the development of liver fibrosis. Met expression in hepatocytes suppressed pro-fibrogenic programs involved in inflammatory cell trafficking, cytoskeletal network reorganization, cell proliferation and DNA damage and stress response.[21] Similarly, recombinant HGF and HGF gene therapy, was shown to attenuate liver fibrosis onset and progression.[64–67] In clinical trials, activation of the HGF/Met signaling axis has been shown to be safe and effective in improving multiple diseases and conditions, including fulminant hepatitis, liver failure, diabetic neuropathy and critical limb ischemia.[68–72] Here, we demonstrate the potential therapeutic role of the MSP/Ron receptor axis for treatment of liver fibrosis.

## CONCLUSIONS

In conclusion, this study highlights the protective role of Ron in liver fibrosis development and progression in a diet-induced NASH model (Figure 6). Because DKO animals harbor a targeted deletion in the ligand binding domain of Ron in all cells, further investigation involving conditional Ron knockout mouse models is necessary to delineate the specific antifibrotic effects of Ron in vivo. In past efforts, we have extensively explored the in vitro and in vivo anti-inflammatory actions of Ron on tissue resident macrophage function including Kupffer cells, which are major drivers of the NASH spectrum. The diet-induced NASH model, although it simulates human NASH, does not pinpoint whether the mitigated liver fibrosis is due to improved steatohepatitis or a direct consequence of Ron-regulated fibrogenic signaling pathways. Hence, further experimentation is required to elucidate how Ron impacts liver fibrosis pathways in key fibrogenic cells including HSCs. Our results suggest that the MSP/Ron signaling axis may be a viable therapeutic target for the treatment of steatohepatitis-induced liver fibrosis.

## Supplementary Material

Refer to Web version on PubMed Central for supplementary material.

## ACKNOWLEDGMENTS

We thank the Animal Diagnostic Laboratories at Pennsylvania State University for hematoxylin & eosin staining of livers. We thank Dr. Joy Pate and Camilla Hughes for the bright field microscopy resources and technical assistance. A sincere thank you to Katy Sanon for diligent proofreading of this manuscript. This research was supported by the Department of Veterinary and Biomedical Sciences of the Pennsylvania State University, the Alfred P. Sloan Foundation Graduate University Centers for Exemplary Mentoring (UCEM) Scholarship, the National Institute of Allergy and Infectious Diseases (NIAID) training in Animal Models of Inflammation Award [2T32AI074551–06] and the National Center for Advancing Translational Sciences (NCATS) Clinical and Translation Science (CTSA) Award [TL1TR002016]

Author Manuscript Author Manuscript Author Manuscript Author Manuscript

## REFERENCES


(1). Michelotti GA; Machado MV; Diehl AM NAFLD, NASH and liver cancer. Nat. Rev. Gastroenterol. Hepatol 2013, 10, 656. [PubMed: 24080776]

(2). Rinella ME Nonalcoholic fattyliver disease: a systematic review. Jama 2015, 313 (22), 2263–73. [PubMed: 26057287]

(3). Koyama Y; Brenner DA Liver inflammation and fibrosis. J. Clin. Invest 2017, 127 (1), 55–64. [PubMed: 28045404]

(4). Evans CDJ; Oien KA; MacSween RNM; Mills PR Non-alcoholic steatohepatitis: a common cause of progressive chronic liver injury? J. Clin. Pathol 2002, 55 (9), 689–692. [PubMed: 12195000]

(5). Haflidadottir S; Jonasson JG; Norland H; Einarsdottir SO; Kleiner DE; Lund SH; Bjornsson ES Long-term follow-up and liver-related death rate in patients with non-alcoholic and alcoholic related fatty liver disease. BMC Gastroenterol. 2014, 14, 166. [PubMed: 25260964]

(6). Stal P Liver fibrosis in non-alcoholic fatty liver disease - diagnostic challenge with prognostic significance. World J. Gastroenterol 2015, 21 (39), 11077–87. [PubMed: 26494963]

(7). Dulai PS; Singh S; Patel J; Soni M; Prokop LJ; Younossi Z; Sebastiani G; Ekstedt M; Hagstrom H; Nasr P; Stal P; Wong VW; Kechagias S; Hultcrantz R; Loomba R Increased risk of mortality by fibrosis stage in nonalcoholic fatty liver disease: Systematic review and meta-analysis. Hepatology 2017, 65 (5), 1557–1565. [PubMed: 28130788]

(8). Hagstrom H; Nasr P; Ekstedt M; Hammar U; Stal P; Hultcrantz R; Kechagias S Fibrosis stage but not NASH predicts mortality and time to development of severe liver disease in biopsy-proven NAFLD. J. Hepatol 2017, 67 (6), 1265–1273. [PubMed: 28803953]

(9). Unalp-Arida A; Ruhl CE Liver fibrosis scores predict liver disease mortality in the United States population. Hepatology 2017, 66 (1), 84–95. [PubMed: 28195363]

(10). Liu QP; Fruit K; Ward J; Correll PH Negative regulation of macrophage activation in response to IFN-gamma and lipopolysaccharide by the STK/RON receptor tyrosine kinase. J. Immunol 1999, 163 (12), 6606–13. [PubMed: 10586055]

(11). Ray M; Yu S; Sharda DR; Wilson CB; Liu Q; Kaushal N; Prabhu KS; Hankey PA Inhibition of TLR4-Induced NF-κB Kinase Activity by the RON Receptor Tyrosine Kinase and Its Ligand, Macrophage-Stimulating Protein. J. Immunol 2010, 185 (12), 7309–7316. [PubMed: 21078906]

(12). Sharda DR; Yu S; Ray M; Squadrito ML; De Palma M; Wynn TA; Morris SM Jr.; Hankey PA Regulation of macrophage arginase expression and tumor growth by the Ron receptor tyrosine kinase. J. Immunol 2011, 187 (5), 2181–92. [PubMed: 21810604]

(13). Wang MH; Zhou YQ; Chen YQ Macrophage-Stimulating Protein and RON Receptor Tyrosine Kinase: Potential Regulators of Macrophage Inflammatory Activities. Scand. J. Immunol 2002, 56 (6), 545–553. [PubMed: 12472665]

(14). Yu S; Allen JN; Dey A; Zhang L; Balandaram G; Kennett MJ; Xia M; Xiong N; Peters JM; Patterson A; Hankey-Giblin PA The Ron Receptor Tyrosine Kinase Regulates Macrophage Heterogeneity and Plays a Protective Role in Diet-Induced Obesity, Atherosclerosis, and Hepatosteatosis. J. Immunol 2016, 197 (1), 25665.

(15). Zhou YQ; Chen YQ; Fisher JH; Wang MH Activation of the RON receptor tyrosine kinase by macrophage-stimulating protein inhibits inducible cyclooxygenase-2 expression in murine macrophages. J. Biol. Chem 2002, 277 (41), 38104–10. [PubMed: 12177064]

(16). Wilson CB; Ray M; Lutz M; Sharda D; Xu J; Hankey PA The RON receptor tyrosine kinase regulates IFN-gamma production and responses in innate immunity. J. Immunol 2008,181 (4), 2303–10. [PubMed: 18684919]

(17). Chaudhuri A; Xie MH; Yang B; Mahapatra K; Liu J; Marsters S; Bodepudi S; Ashkenazi A Distinct involvement of the Gab1 and Grb2 adaptor proteins in signal transduction by the related receptor tyrosinekinases RON and MET. J. Biol. Chem 2011,286 (37), 32762–74. [PubMed: 21784853]

(18). Schaeper U; Gehring NH; Fuchs KP; Sachs M; Kempkes B; Birchmeier W Coupling of Gab1 to c-Met, Grb2, and Shp2 mediates biological responses. J. Cell Biol 2000, 149 (7), 1419–32. [PubMed: 10871282]

Author Manuscript Author Manuscript Author Manuscript Author Manuscript

(19). Finkelstein LD; Ney PA; Liu QP; Paulson RF; Correll PH Sf-Stk kinase activityand the Grb2 bindingsite are required for Epo-independent growth of primary erythroblasts infected with Friend virus. Oncogene 2002, 21 (22), 3562–70. [PubMed: 12032858]

(20). Kizu T; Yoshida Y; Furuta K; Ogura S; Egawa M; Chatani N; Hamano M; Takemura T; Ezaki H; Kamada Y; Nishida K; Nakaoka Y; Kiso S; Takehara T Loss of Gab1 adaptor protein in hepatocytes aggravates experimental liver fibrosis in mice. Am. J. Physiol Gastrointest Liver Physiol 2015, 308 (7), G613–24. [PubMed: 25617348]

(21). Giebeler A; Boekschoten MV; Klein C; Borowiak M; Birchmeier C; Gassler N; Wasmuth HE; Muller M; Trautwein C; Streetz KL c-Met confers protection against chronic liver tissue damage and fibrosis progression after bile duct ligation in mice. Gastroenterology 2009, 137 (1), 297–308. [PubMed: 19208365]

(22). Kroy DC; Schumacher F; Ramadori P; Hatting M; Bergheim I; Gassler N; Boekschoten MV; Muller M; Streetz KL; Trautwein C Hepatocyte specific deletion of c-Met leads to the development of severe non-alcoholic steatohepatitis in mice. J. Hepatol 2014, 61 (4), 883–90. [PubMed: 24845607]

(23). Zhang L; Hatzakis E; Nichols RG; Hao R; Correll J; Smith PB; Chiaro CR; Perdew GH; Patterson AD Metabolomics Reveals that Aryl Hydrocarbon Receptor Activation by Environmental Chemicals Induces Systemic Metabolic Dysfunction in Mice. Environ. Sci. Technol 2015, 49 (13), 8067–77. [PubMed: 26023891]

(24). Belton KR; Tian Y; Zhang L; Anitha M; Smith PB; Perdew GH; Patterson AD Metabolomics Reveals Aryl Hydrocarbon Receptor Activation Induces Liver and Mammary Gland Metabolic Dysfunction in Lactating Mice. J. Proteome Res 2018, 17 (4), 1375–1382. [PubMed: 29521512]

(25). Bezerra JA; Laney DW; Degen SJF Increased Expression of mRNA for Hepatocyte Growth Factor-like Protein during Liver Regeneration and Inflammation. Biochem. Biophys. Res. Commun 1994, 203 (1), 666–673. [PubMed: 8074719]

(26). Böhm F; Köhler UA; Speicher T; Werner S Regulation of liver regeneration by growth factors and cytokines. EMBO Molecular Medicine 2010, 2 (8), 294–305. [PubMed: 20652897]

(27). Shiota G; Okano J-I; Kawasaki H; Kawamoto T; Nakamura T Serum hepatocyte growth factor levels in liver diseases: Clinical implications. Hepatology 1995, 21 (1), 106–112. [PubMed: 7806142]

(28). Hernandez-Gea V; Friedman SL Pathogenesis of Liver Fibrosis. Annu. Rev. Pathol.: Mech. Dis 2011, 6 (1), 425–456.

(29). Bataller R; Brenner DA Liver fibrosis. J. Clin. Invest 2005, 115 (2), 209–18. [PubMed: 15690074]

(30). Xu R; Zhang Z; Wang F-S Liver fibrosis: mechanisms of immune-mediated liver injury. Cell. Mol. Immunol. 2012, 9, 296. [PubMed: 22157623]

(31). Elpek GÖ Cellular and molecular mechanisms in the pathogenesis of liver fibrosis: An update. World Journal of Gastroenterology: WJG 2014, 20 (23), 7260–7276. [PubMed: 24966597]

(32). Moreira RK Hepatic stellate cells and liver fibrosis. Arch. Pathol. Lab. Med 2007, 131 (11), 1728–34. [PubMed: 17979495]

(33). Tsukamoto H Cytokine regulation of hepatic stellate cells in liver fibrosis. Alcohol.: Clin. Exp. Res 1999, 23 (5), 911–6. [PubMed: 10371413]

(34). De Minicis S; Seki E; Uchinami H; Kluwe J; Zhang Y; Brenner DA; Schwabe RF Gene expression profiles during hepatic stellate cell activation in culture and in vivo. Gastroenterology 2007,132 (5), 1937–46. [PubMed: 17484886]

(35). Ju C; Tacke F Hepatic macrophages in homeostasis and liver diseases: from pathogenesis to novel therapeutic strategies. Cell. Mol. Immunol 2016, 13 (3), 316–327. [PubMed: 26908374]

(36). Pradere J-P; Kluwe J; De Minicis S; Jiao J-J; Gwak G-Y; Dapito DH; Jang M-K; Guenther ND; Mederacke I; Friedman R; Dragomir A-C; Aloman C; Schwabe RF Hepatic macrophages but not dendritic cells contribute to liver fibrosis by promoting the survival of activated hepatic stellate cells in mice. Hepatology 2013, 58 (4), 1461–1473. [PubMed: 23553591]

(37). Seki E; Schwabe RF Hepatic inflammation and fibrosis: functional links and key pathways. Hepatology 2015, 61 (3), 1066–79. [PubMed: 25066777]

Author Manuscript Author Manuscript Author Manuscript Author Manuscript

(38). Tacke F; Zimmermann HW Macrophage heterogeneity in liver injury and fibrosis. J. Hepatol 2014, 60 (5), 1090–6. [PubMed: 24412603]

(39). Wynn TA; Barron L Macrophages: master regulators of inflammation and fibrosis. Semin. Liver Dis 2010, 30 (3), 245–57. [PubMed: 20665377]

(40). Wynn TA; Vannella KM Macrophages in tissue repair, regeneration, and fibrosis. Immunity 2016, 44 (3), 450–462. [PubMed: 26982353]

(41). Gitto S; Schepis F; Andreone P; Villa E, Study of the serum metabolomic profile in nonalcoholic fatty liver disease: Research and clinical perspectives. Metabolites 2018, 8, (1).17

(42). Nielsen J Systems Biology of Metabolism: A Driver for Developing Personalized and Precision Medicine. Cell Metab 2017, 25 (3), 572–579. [PubMed: 28273479]

(43). Mardinoglu A; Agren R; Kampf C; Asplund A; Uhlen M; Nielsen J Genome-scale metabolic modelling of hepatocytes reveals serine deficiency in patients with non-alcoholic fatty liver disease. Nat. Commun 2014, 5, 3083. [PubMed: 24419221]

(44). Mardinoglu A; Bjornson E; Zhang C; Klevstig M; Soderlund S; Stahlman M; Adiels M; Hakkarainen A; Lundbom N; Kilicarslan M; Hallstrom BM; Lundbom J; Verges B; Barrett PH; Watts GF; Serlie MJ; Nielsen J; Uhlen M; Smith U; Marschall HU; Taskinen MR; Boren J Personal model-assisted identification of NAD(+) and glutathione metabolism as intervention target in NAFLD. Mol. Syst. Biol 2017, 13 (3), 916. [PubMed: 28254760]

(45). Gaggini M; Carli F; Rosso C; Buzzigoli E; Marietti M; Della Latta V; Ciociaro D; Abate ML; Gambino R; Cassader M; Bugianesi E; Gastaldelli A Altered amino acid concentrations in NAFLD: Impact of obesity and insulin resistance. Hepatology 2018, 67 (1), 145–158. [PubMed: 28802074]

(46). Rivera CA; Bradford BU; Hunt KJ; Adachi Y; Schrum LW; Koop DR; Burchardt ER; Rippe RA; Thurman RG Attenuation of CCl4-induced hepatic fibrosis by GdCl3 treatment or dietary glycine. American Journal ofPhysiology-Gastrointestinal and Liver Physiology 2001, 281 (1), G200–G207.

(47). Senthilkumar R; Nalini N Glycine prevents hepatic fibrosis by preventing the accumulation of collagen in rats with alcoholic liver injury. Pol. J. Pharmacol 2004, 56 (1), 121–8. [PubMed: 15047986]

(48). Zhou X; Han D; Xu R; Wu H; Qu C; Wang F; Wang X; Zhao Y Glycine protects against high sucrose and high fat-induced non-alcoholic steatohepatitis in rats. Oncotarget 2016, 7 (49), 80223–80237. [PubMed: 27784003]

(49). Yamashina S; Ikejima K; Enomoto N; Takei Y; Sato N Glycine as a therapeutic immuno-nutrient for alcoholic liver disease. Alcohol.: Clin. Exp. Res 2005, 29 (11 Suppl), 162s–5s. [PubMed: 16344603]

(50). Linton MF; Yancey PG; Davies SS; Jerome WGJ; Linton EF; Vickers KC The Role of Lipids and Lipoproteins in Atherosclerosis. In De Groot LJ; Chrousos G; Dungan K; Feingold KR; Grossman A; Hershman JM; Koch C; Korbonits M; McLachlan R; New M; Purnell J; Rebar R; Singer F; Vinik A, Eds.; MDText.com, Inc.: South Dartmouth (MA), 2000.

(51). Dallas SL; Sivakumar P; Jones CJ; Chen Q; Peters DM; Mosher DF; Humphries MJ; Kielty CM Fibronectin regulates latent transforming growth factor-beta (TGF beta) by controlling matrix assembly of latent TGF beta-binding protein-1. J. Biol. Chem 2005, 280 (19), 18871–80. [PubMed: 15677465]

(52). Kawelke N; Vasel M; Sens C; Au A; Dooley S; Nakchbandi IA Fibronectin protects from excessive liver fibrosis by modulating the availability of and responsiveness of stellate cells to active TGF-beta. PLoS One 2011, 6 (11), e28181. [PubMed: 22140539]

(53). Duarte S; Baber J; Fujii T; Coito AJ Matrix metalloproteinases in liver injury, repair and fibrosis. Matrix Biol. 2015, 44–46, 147–56. [PubMed: 25599939]

(54). Han YP Matrix metalloproteinases, the pros and cons, in liver fibrosis. J. Gastroenterol. Hepatol 2006, 21 (Suppl 3), S88–91. [PubMed: 16958682]

(55). Hemmann S; Graf J; Roderfeld M; Roeb E Expression of MMPs and TIMPs in liver fibrosis - a systematic review with special emphasis on anti-fibrotic strategies. J. Hepatol 2007, 46 (5), 955–75. [PubMed: 17383048]

Author Manuscript Author Manuscript Author Manuscript Author Manuscript

(56). Atta H; El-Rehany M; Hammam O; Abdel-Ghany H; Ramzy M; Roderfeld M; Roeb E; Al-Hendy A; Raheim SA; Allam H; Marey H Mutant MMP-9 and HGF gene transfer enhance resolution of CCl4-induced liver fibrosis in rats: role of ASH1 and EZH2 methyltransferases repression. PLoS One 2014, 9 (11), e112384. [PubMed: 25380300]

(57). Roderfeld M; Weiskirchen R; Wagner S; Berres ML; Henkel C; Grotzinger J; Gressner AM; Matern S; Roeb E Inhibition of hepatic fibrogenesis by matrix metalloproteinase-9 mutants in mice. FASEB J. 2006, 20 (3), 444–54. [PubMed: 16507762]

(58). Cabrera S; Gaxiola M; Arreola JL; Ramirez R; Jara P; D'Armiento J; Richards T; Selman M; Pardo A Overexpression of MMP9 in macrophages attenuates pulmonary fibrosis induced by bleomycin. Int. J. Biochem. Cell Biol 2007, 39 (12), 2324–38. [PubMed: 17702637]

(59). Zhou X; Murphy FR; Gehdu N; Zhang J; Iredale JP; Benyon RC Engagement of **avfi3** Integrin Regulates Proliferation and Apoptosis of Hepatic Stellate Cells. J. Biol. Chem 2004, 279 (23), 23996–24006. [PubMed: 15044441]

(60). Dixon LJ; Barnes M; Tang H; Pritchard MT; Nagy LE Kupffer cells in the liver. Compr Physiol 2013, 3 (2), 785–97. [PubMed: 23720329]

(61). Bilzer M; Roggel F; Gerbes AL Role of Kupffer cells in host defense and liver disease. Liver Int. 2006, 26 (10), 1175–86. [PubMed: 17105582]

(62). Li H; You H; Fan X; Jia J Hepatic macrophages in liver fibrosis: pathogenesis and potential therapeutic targets. BMJ. Open Gastroenterology 2016, 3 (1), e000079.

(63). Itoh M; Suganami T; Kato H; Kanai S; Shirakawa I; Sakai T; Goto T; Asakawa M; Hidaka I; Sakugawa H; Ohnishi K; Komohara Y; Asano K; Sakaida I; Tanaka M; Ogawa Y, CD11c+ resident macrophages drive hepatocyte death-triggered liver fibrosis in a murine model of nonalcoholic steatohepatitis. JCI Insight 2017, 2, (22). DOI: 10.1172/jci.insight.92902

(64). Matsuda Y; Matsumoto K; Ichida T; Nakamura T Hepatocyte growth factor suppresses the onset of liver cirrhosis and abrogates lethal hepatic dysfunction in rats. J. Biochem 1995, 118 (3), 643–9. [PubMed: 8690730]

(65). Xia J-L; Dai C; Michalopoulos GK; Liu Y Hepatocyte Growth Factor Attenuates Liver Fibrosis Induced by Bile Duct Ligation. Am. J. Pathol 2006, 168 (5), 1500–1512. [PubMed: 16651617]

(66). Matsuda Y; Matsumoto K; Yamada A; Ichida T; Asakura H; Komoriya Y; Nishiyama E; Nakamura T Preventive and therapeutic effects in rats of hepatocyte growth factor infusion on liver fibrosis/cirrhosis. Hepatology 1997, 26 (1), 81–9. [PubMed: 9214455]

(67). Sato M; Kakubari M; Kawamura M; Sugimoto J; Matsumoto K; Ishii T The decrease in total collagen fibers in the liver by hepatocyte growth factor after formation of cirrhosis induced by thioacetamide. Biochem. Pharmacol 2000, 59 (6), 681–90. [PubMed: 10677585]

(68). Ido A; Moriuchi A; Numata M; Murayama T; Teramukai S; Marusawa H; Yamaji N; Setoyama H; Kim ID; Chiba T; Higuchi S; Yokode M; Fukushima M; Shimizu A; Tsubouchi H Safety and pharmacokinetics of recombinant human hepatocyte growth factor (rh-HGF) in patients with fulminant hepatitis: a phase I/II clinical trial, following preclinical studies to ensure safety. J. Transl Med 2011, 9, 55. [PubMed: 21548996]

(69). Cui YL; Meng MB; Tang H; Zheng MH; Wang YB; Han HX; Lei XZ Recombinant human hepatocyte growth factor for liver failure. Contemp. Clin. Trials 2008, 29 (5), 696–704. [PubMed: 18554990]

(70). Nakamura T; Mizuno S The discovery of hepatocyte growth factor (HGF) and its significance for cell biology, life sciences and clinical medicine. Proc. Jpn. Acad., Ser. B 2010, 86 (6), 588–610. [PubMed: 20551596]

(71). Shigematsu H; Yasuda K; Iwai T; Sasajima T; Ishimaru S; Ohashi Y; Yamaguchi T; Ogihara T; Morishita R Randomized, double-blind, placebo-controlled clinical trial of hepatocyte growth factor plasmid for critical limb ischemia. Gene Ther. 2010, 1152–61. [PubMed: 20393508]

(72). Kessler JA; Smith AG; Cha BS; Choi SH; Wymer J; Shaibani A; Ajroud-Driss S; Vinik A Double-blind, placebocontrolled study of HGF gene therapy in diabetic neuropathy. Ann. Clin. Transl. Neurol 2015, 2 (5), 465–78. [PubMed: 26000320]

Author Manuscript Author Manuscript Author Manuscript Author Manuscript

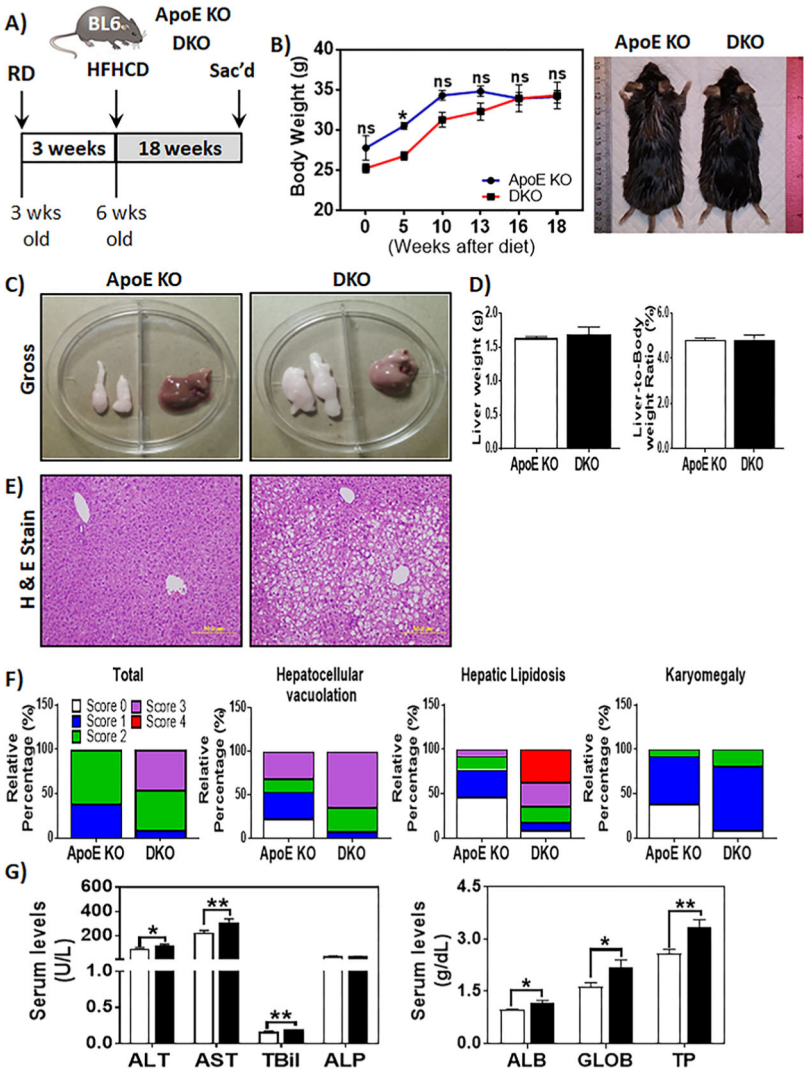


**Figure 1.**

Increased hepatic damage in HFHCD-fed ApoE KO mice with impaired Ron signaling. (A) Scheme of experimental design shown. Six-week-old mice were maintained on a HFHCD for 18 weeks. (B) Measured body weights of HFHCD-fed animals at indicated time points ($n$ = 12–16 per group, two-way ANOVA followed by a Bonferroni's posttest). (C) Representative images of gross liver morphology for diet-fed ApoE KO and DKO mice. (D) Liver weights of ApoE KO and DKO mice maintained on a HFHC diet for 18 weeks ($n$ = 6 per group). (E) Representative images that show liver cross sections stained with hematoxylin and eosin (Scale bar = 100 $\mu$m). (F) Histological scoring of H&E stained livers from ApoE KO and DKO mice ($n$ = 12 per group). (G) Serum levels of alanine transaminase (ALT), aspartate transaminase (AST), total bilirubin (TBIL), alkaline phosphatase (ALP), albumin (ALB), globulin (GLOB), and total protein (TP) in HFHCD-fed mice ($n$ = 12–16 per group). Data are depicted as mean ± SEM and degree of statistical significance is presented as $^{*}p < 0.05$, ** $p < 0.01$.

Author Manuscript Author Manuscript Author Manuscript Author Manuscript

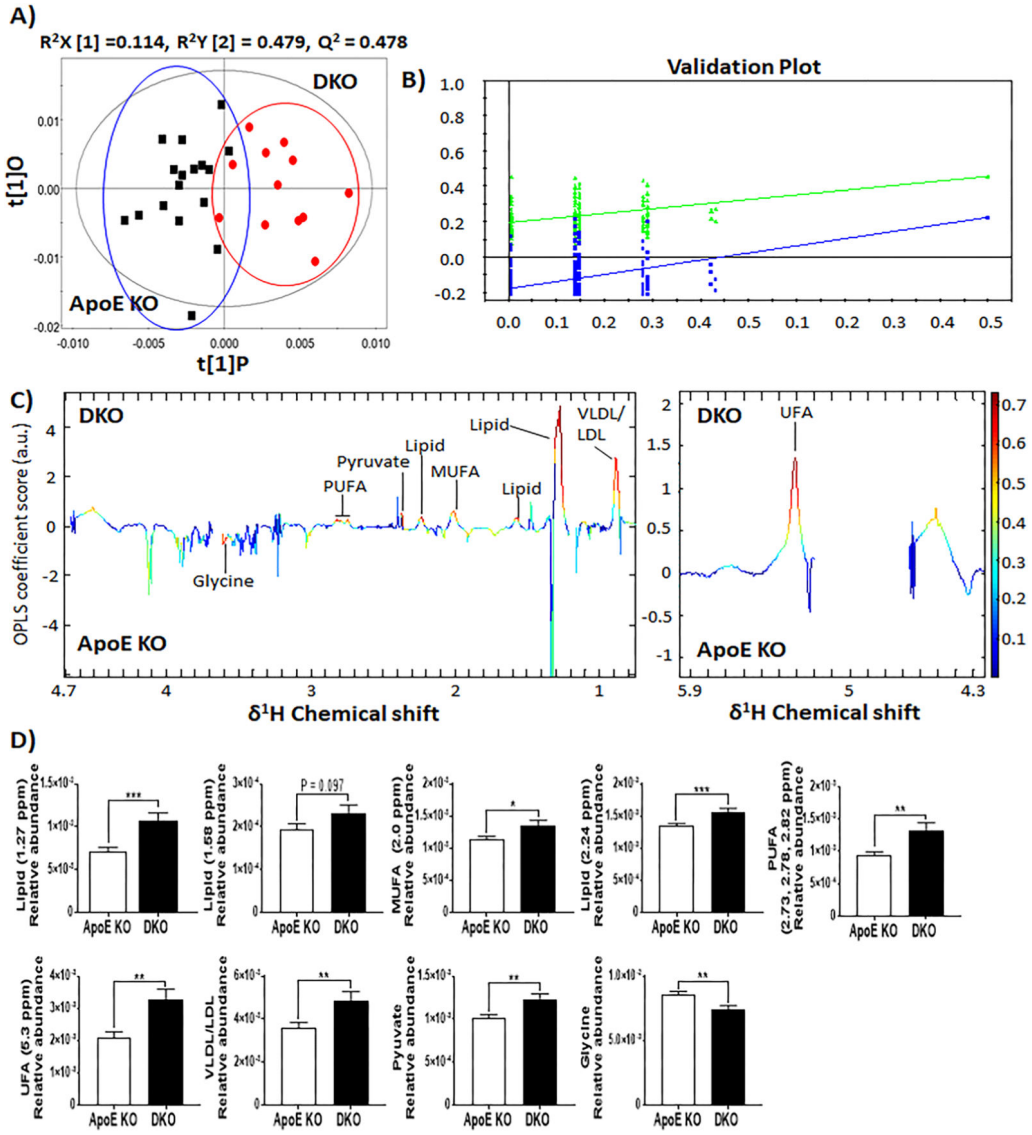


**Figure 2.**

Increased levels of circulating lipids and serological markers of liver disease in HFHCD -fed ApoE KO mice with impaired Ron receptor signaling. (A) OPLS-DA score plot of metabolite profiles on $^{1}$H NMR spectra of blood sera derived from HFHCD-fed mice. Each red and black circle represents one $^{1}$H CPMG NMR of serum of a DKO and an ApoE KO mouse, respectively. (B) Validation plot of the OPLS-DA score plot for HFHCD-fed ApoE KO ($n$ = 17) and DKO ($n$ = 12) groups generated using 7-fold cross validation method. (C) OPLS-DA color-coded coefficient plot of sera obtained from HFHC diet-fed ApoE KO and DKO mice. The upward orientation of the peaks denotes higher concentration of the metabolite in the corresponding group of HFHCD-fed mice. The color of the signals signifies the strength of relationship between the metabolite and corresponding HFHCD-fed mouse group with red representing highest significance and blue representing least significance. (D) Vertical bar graphs of significant $^{1}$H NMR metabolites. Bar graphs

represent the data as mean ± SEM and degree of statistical significance is presented as *$p <$ 0.05, ** $p < 0.01$, *** $p < 0.001$.

Author Manuscript Author Manuscript Author Manuscript Author Manuscript

Author Manuscript Author Manuscript Author Manuscript Author Manuscript

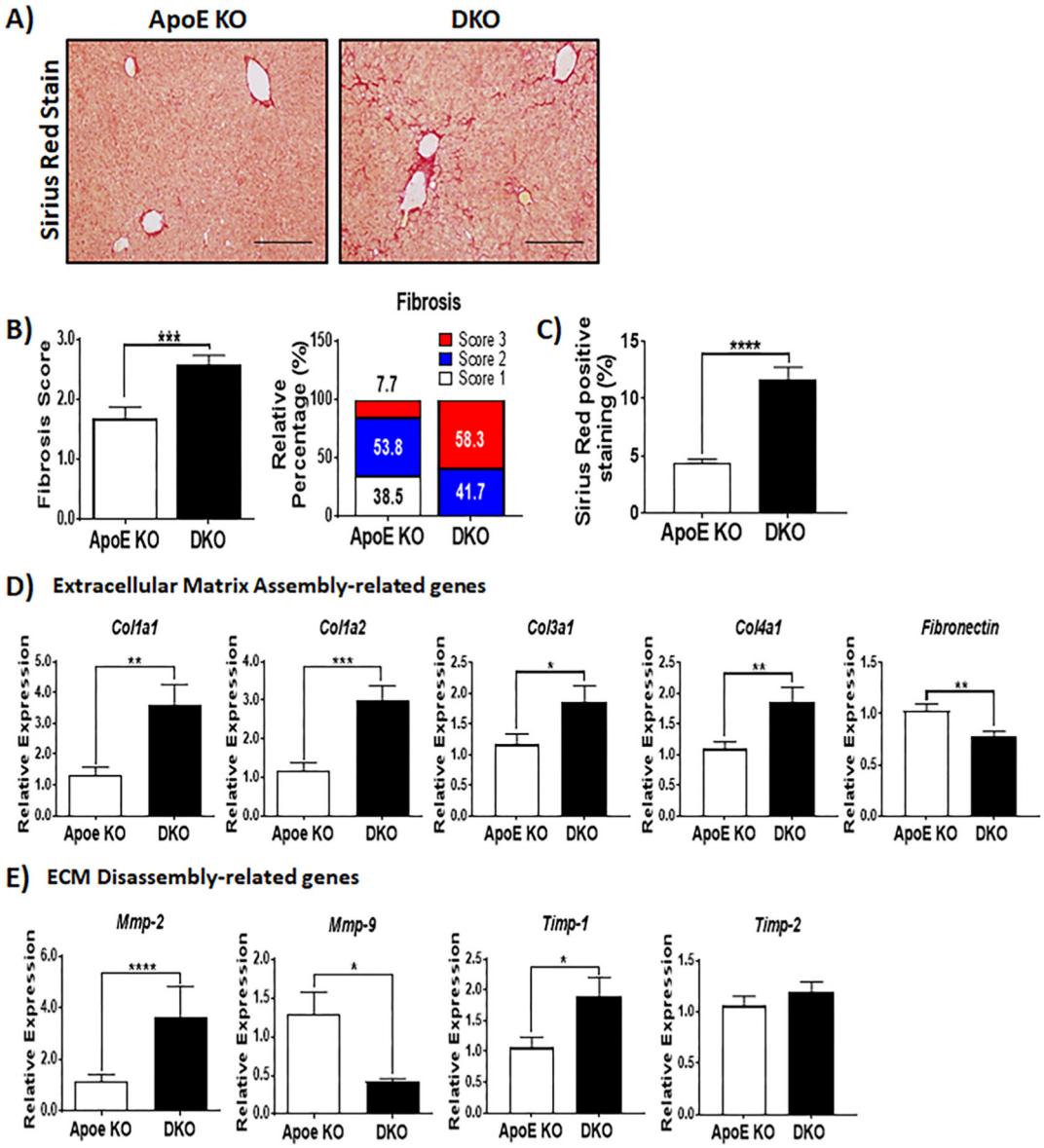


**Figure 3.**

Ron receptor deficiency results in increased expression of genes involved in extracellular matrix remodeling and collagen deposition. (A and B) Histomorphological analysis assessing the stage of liver fibrosis using standard scoring index (Score 1 = normal to minimal fibrosis, 2 = mild fibrosis, 3 = moderate fibrosis), $n = 12$ per group. (C) Quantitative analysis of Sirius red stained collagen accumulation in ApoE KO and DKO livers ($n = 12$ per group). (D) Expression levels of genes involved in ECM assembly including collagen type 1 (*Col1a1, Col1a2*), collagen type 3 (*Col3a1*), collagen type 4 (*Col4a1*), and fibronectin. (E) Gene expression of ECM disassembly-related genes such as matrix metalloproteinase-2 *(Mmp-2)*, matrix metalloproteinase-9 *(Mmp-9)*, tissue inhibitor of metalloproteinase —1 *(Timp-1)*, and tissue inhibitor of metalloproteinase-2 *(Timp-2)*. Graphs depict the data as mean ± SEM ($n = 12$—16 per group). Statistical significance was presented as $*p < 0.05$, ** $p < 0.01$, *** $p < 0.001$, **** $p < 0.0001$.

Author Manuscript Author Manuscript Author Manuscript Author Manuscript

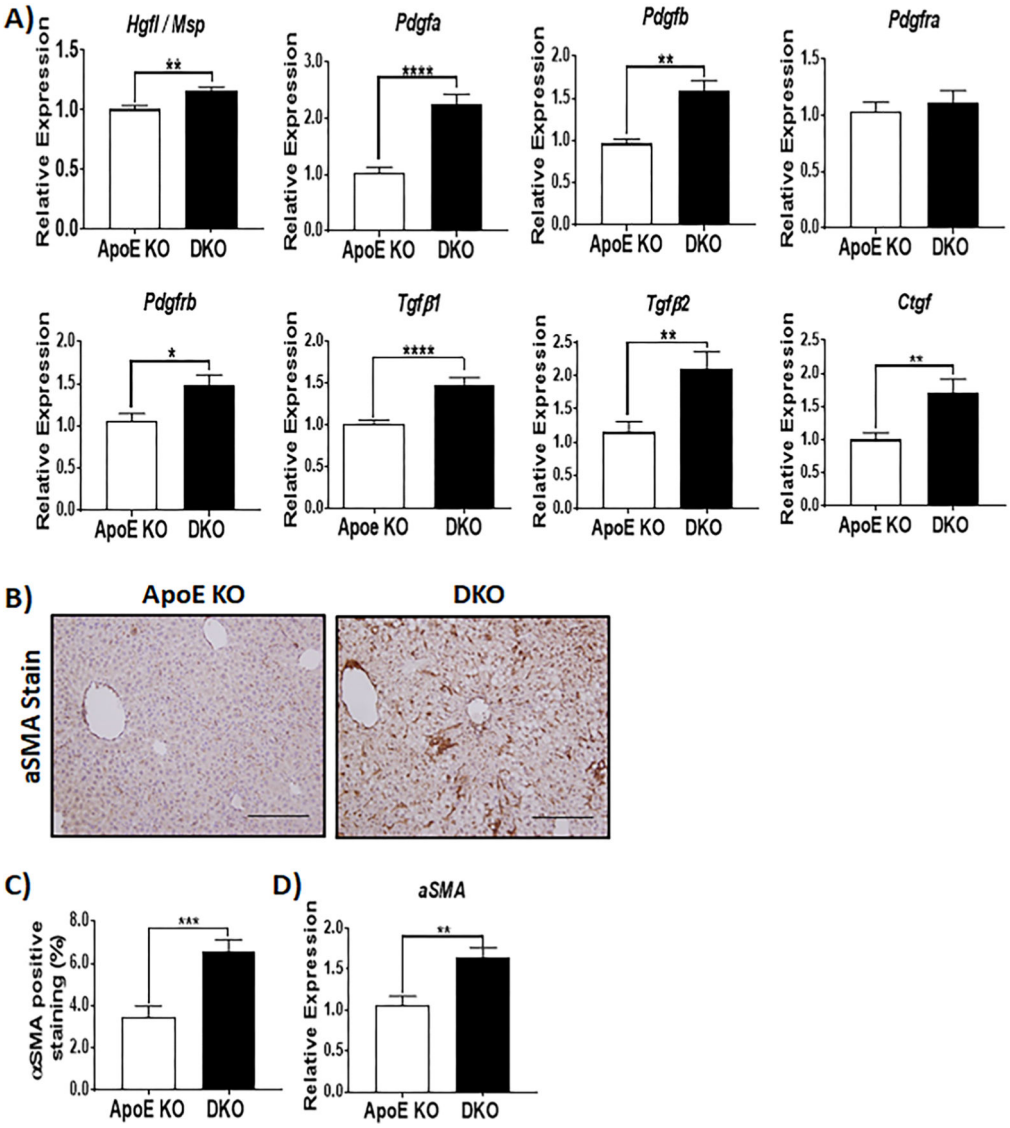


**Figure 4.**

Deficiency in the Ron receptor augments the expression of MSP, pro-fibrogenic cytokines and hepatic stellate cell activation. (A) Transcript levels of *Msp (Hgfl)* and pro-fibrogenic cytokines/receptors such as *Tgfβ, Pdgfα, Pdgfβ Pdgfrα, Pdgfrβ*, and *Ctgf* in livers from ApoE KO and DKO mice maintained on a HFHCD for 18 weeks ($n$ = 12–16 per group. (B) Photomicrograph of αSMA immunostained livers from HFHC diet-fed animal. Scale bar represents 100 μm. (C) Quantitative analysis of αSMA positive area (%) in fibrotic livers from mice on a HFHCD ($n$ = 10 per group). (D) Gene expression of αSMA in the liver determined by quantitative RT-PCR (mean ± SEM; $n$ = 12–16 per group). Statistical significance was presented as *$p < 0.05$, ** $p < 0.01$, *** $p < 0.001$, or **** $p < 0.0001$.

Author Manuscript
Author Manuscript
Author Manuscript
Author Manuscript



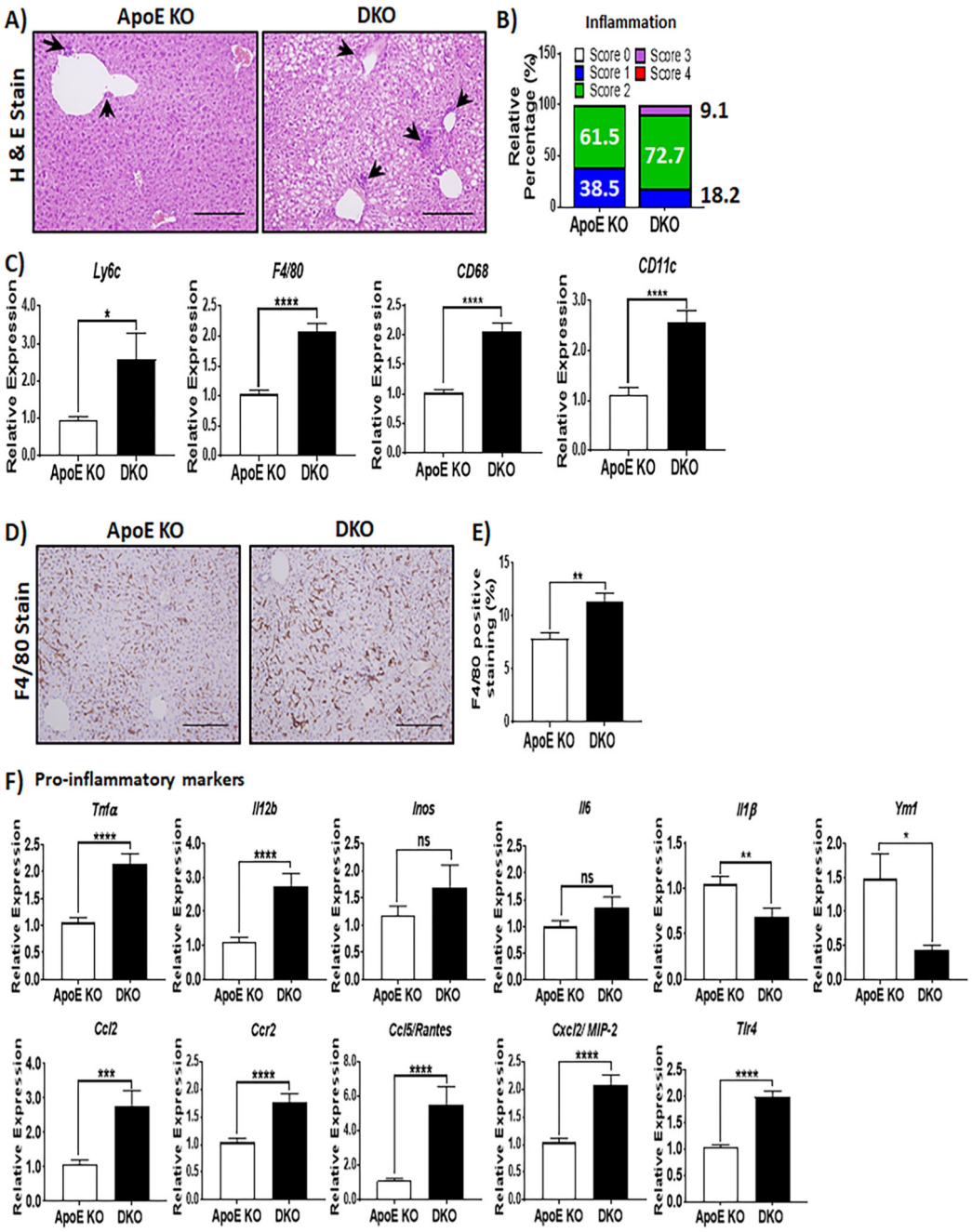


**Figure 5.**

Increased immune cell recruitment and inflammation in livers of HFHCD-fed DKO animals. (A) Representative H&E histology photomicrographs of immune cell infiltrates in livers shown by black arrows. (B) Inflammation index for livers from ApoE KO and DKO mice maintained on a HFHC diet for 18 weeks ($n$ = 12per group). (C) Gene expression of immune cell markers determined by quantitative RT-PCR ($n$ = 12–16 per group). (D) Representative F4/80 immunohistochemistry (IHC) images and (E) quantification of F4/80 positive areas (%), $n$ = 8 per group. (F) Gene expression of the pro-inflammatory markers *Tnfa, Il-12b, Inos, Il-1β, Il-6* and *Tlr4* and anti-inflammatory marker *Ym-1,* as well as the chemokines/

Author Manuscript Author Manuscript Author Manuscript Author Manuscript

chemokine receptors *Cxcl2* or *Mip2, Ccl2, Ccr2,* and *Ccl5* or *Rantes* evaluated by quantitative RT-PCR. The data presented as mean ± SEM ($n$ = 12–16 per group), * $p < 0.05$, ** $p < 0.01$, *** $p < 0.001$, **** $p < 0.0001$.

Author Manuscript Author Manuscript Author Manuscript Author Manuscript

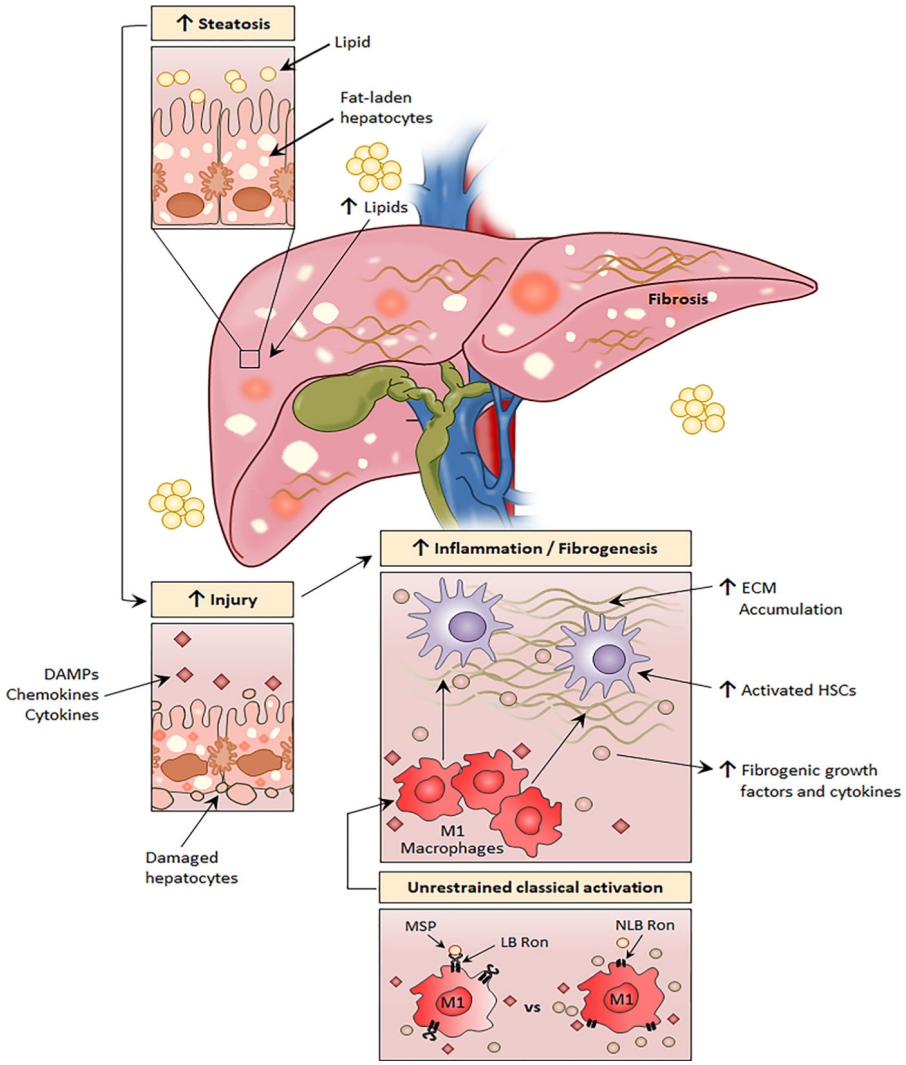


**Figure 6.**

Schematic depiction of hepatic fibrosis exacerbation in DKO mice. In response to a high fat high cholesterol diet, DKO mice exhibit increased circulating levels oflipids. The higher circulating concentrations of lipids contribute to accelerated hepatic steatosis development. The fat-laden hepatocytes sustain exacerbated cellular damage, releasing greater amounts of chemokines, cytokines and danger-associated molecular patterns (DAMPs) that recruit and classically activate macrophage. In DKO mice, the Ron receptor lacks the ligand-binding domain resulting in cells that are incapable of being stimulated by the Ron receptor ligand, macrophage stimulating protein (MSP). Consequently, MSP cannot exert its anti-inflammatory effects on inflammatory cells including liver macrophages. Hepatic macrophages lacking the ligand binding domain of the Ron receptor, in the presence of inflammatory stimuli, undergo unrestrained classical (M1) activation and secrete greater amounts of fibrogennic inflammatory mediators. The aggravated inflammatory response, in turn, stimulates the activation, proliferation, and survival of neighboring hepatic stellate cells. Activated hepatic stellate cells transdifferentiate into fibrogenic myofibroblast-like

Author Manuscript Author Manuscript Author Manuscript Author Manuscript

cells that produce collagen and other extracellular components, resulting in accelerated fibrogenesis and liver fibrosis development. LB = ligand binding; NLB = nonligand binding.